Quantum oscillations and subband properties of the two-dimensional electron gas at the $LaAlO_3/SrTiO_3$ interface

A. McCollam,[1,a] S. Wenderich,[2] M. K. Kruize,[2] V. K. Guduru,[1]
H. J. A. Molegraaf,[2] M. Huijben,[2] G. Koster,[2] D. H. A. Blank,[2] G. Rijnders,[2]
A. Brinkman,[2] H. Hilgenkamp,[2] U. Zeitler,[1] and J. C. Maan[1]
[1]*High Field Magnet Laboratory and Institute for Molecules and Materials, Radboud University Nijmegen, 6525 ED Nijmegen, The Netherlands*
[2]*Faculty of Science and Technology and MESA+ Institute for Nanotechnology, University of Twente, 7500 AE Enschede, The Netherlands*

(Received 14 December 2013; accepted 19 January 2014; published online 4 February 2014)

We have performed high field magnetotransport measurements to investigate the interface electron gas in a high mobility $SrTiO_3/SrCuO_2/LaAlO_3/SrTiO_3$ heterostructure. Shubnikov-de Haas oscillations reveal several 2D conduction subbands with carrier effective masses of $0.9m_e$ and $2m_e$, quantum mobilities of order 2000 cm^2/V s, and band edges only a few millielectronvolts below the Fermi energy. Measurements in tilted magnetic fields confirm the 2D character of the electron gas, and show evidence of inter-subband scattering.
[http://dx.doi.org/10.1063/1.4863786]

It is now well-established that a two-dimensional electron gas (2DEG) can exist at the interface between perovskite oxides $LaAlO_3$ (LAO) and $SrTiO_3$ (STO).[1,2] The 2DEG is nominally similar to those in semiconductor heterostructures, but supports additional phases, such as superconductivity and magnetism, which are not observed in conventional 2D electron systems, and which have great fundamental and technological interest.[3,4] The mechanism of formation of this oxide 2DEG, however, is not established, and although there is a general consensus that the charge carriers occupy STO conduction bands modified by the presence of the interface,[2,5] the origin and density of the 2D carriers, and the details of the electronic bandstructure at the interface are not yet fully understood.

Quantum oscillations in the transport properties of metallic and semiconducting materials arise directly from the magnetic field dependence of the conduction electron energies, and are, therefore, a powerful experimental probe of the electronic bandstructure close to the Fermi energy.[6] They also provide band-specific details of conduction electron properties such as effective mass and mobility. Access to this information in LAO/STO and related heterostructures is highly desirable, as the bandstructure of the 2DEG can be expected to reflect the mechanism of its formation, as well as giving further insight into its behaviour.

Previous quantum oscillation experiments on LAO/STO measured the Shubnikov-de Haas (SdH) effect in the resistivity, and could clearly resolve only a single oscillation frequency corresponding to a single conduction band with high mobility charge carriers.[7–9] In samples with high carrier density (of order 10^{16} cm^{-2}) the oscillations were independent of the magnetic field direction, and indicated a three-dimensional Fermi surface containing all of the charge carriers.[7] These samples were grown under conditions of low oxygen partial pressure ($<10^{-5}$ mbar), and the high carrier density and mobility were believed to arise from uniform doping of the STO substrate by oxygen vacancies.

SdH oscillations were also observed in samples grown or annealed under higher oxygen pressures,[8,9] with low carrier densities of the order of 10^{13} cm^{-2}, thought to be characteristic

[a]Electronic mail: A.McCollam@science.ru.nl

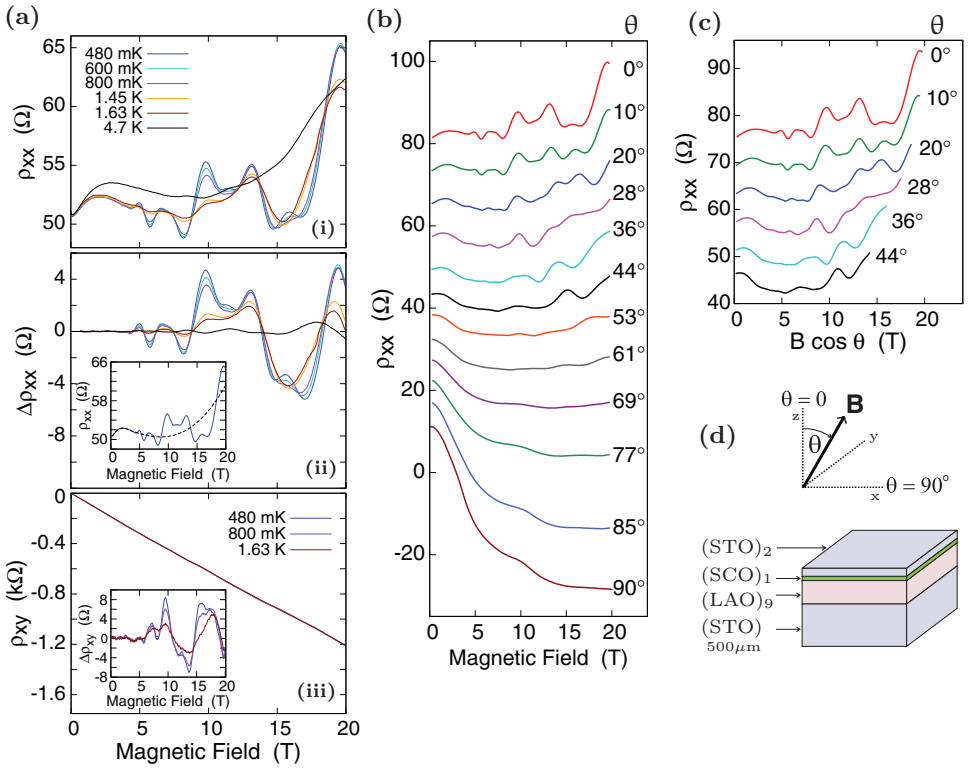

FIG. 1. (a)(i) $\rho_{xx}(B)$ at several different temperatures. (a)(ii) The oscillations in (i) with background removed. An example of the background subtracted is shown as a dashed line in the inset. (a)(iii) Hall effect at different temperatures. The inset shows the quantum oscillations after subtraction of the linear background. (b) Dependence of SdH oscillations on magnetic field orientation. The angle θ between the magnetic field direction and the normal to the interface is shown beside each of the curves, which are offset vertically for clarity. (c) SdH oscillations up to 44° (from (b)), as a function of the perpendicular field component $B\cos\theta$. (d) Sketch of the STO/SCO/LAO/STO structure and field orientation.

of intrinsic samples with few oxygen vacancies. Slightly different values were reported for the SdH frequency but, in both cases, the observed conduction band was two-dimensional with very low carrier density compared to the value of $\sim 10^{13}$ cm^{-2} extracted from the Hall effect (of order 20%). These results raised interesting questions about the presence of conduction channels which do not contribute to the SdH effect, or the possibility of multiple valley and spin degeneracies,[8,9] suggesting that the LAO/STO conduction-bandstructure is considerably more complex than implied by the single observed SdH frequency. A complex bandstructure is also predicted by density-functional calculations, which give a large number of subbands, with quite different carrier properties, crossing the Fermi energy.[10–12]

In this work, we present a detailed magnetotransport investigation of an LAO/STO-based heterostructure, as a function of temperature and in a range of magnetic field orientations, from perpendicular to parallel to the oxide layers. By using very high magnetic fields and a high-mobility 2DEG, we were able to measure well-resolved Shubnikov-de Haas oscillations, and identified and characterised several 2D conduction subbands. Notably, the subbands are separated by only a few millielectronvolts, and have different effective masses and mobilities. In contrast to previous work, we found a relatively high total carrier density of $\sim 0.7 \times 10^{13}$ cm^{-2} contributing to the SdH effect, which is comparable to the carrier density of 10^{13} cm^{-2} extracted from the Hall effect.

Our heterostructure was grown by pulsed laser deposition, with nine monolayers of LAO deposited on a TiO_2-terminated STO(001) substrate. A single monolayer of $SrCuO_2$ (SCO) and two monolayers of STO were grown as capping layers on top of the LAO, as illustrated in Fig. 1(d). Oxygen partial pressure of 2×10^{-3} mbar was used during LAO growth. Full details of the growth procedure and parameters are given as supplementary material.[13] We also carried out

measurements on similar samples with ten monolayers of LAO, and found the results to be consistent with those we report here (see the supplementary material[13]).

The role of the SCO layer is not, at present, fully understood, but we find that it considerably increases the mobility of the LAO/STO interface, compared to samples prepared in an identical way, but without SCO, possibly because the SCO layer acts as a preferential site for oxygen vacancies.[14] We find no evidence of a conducting channel at isolated SCO/LAO or SCO/STO interfaces, and assume that the single monolayer of SCO in our heterostructures does not contribute directly to the conductivity by supporting an additional 2DEG.

It is known that the properties of the LAO/STO interface are highly sensitive to the sample growth conditions,[4,7,15,16] to the thickness and stoichiometry of the LAO layer,[17–20] and to any treatment of the LAO surface.[21,22] It is therefore to be expected that the SCO and STO capping layers affect the interface properties. It was previously shown that one or two STO capping layers significantly modify the bandgap at the LAO/STO interface, and also serve to protect the LAO surface, reducing its sensitivity to defects or adsorbates.[23] We find that, in addition to enhanced mobility, STO/SCO/LAO/STO samples have reduced sensitivity to growth conditions and handling, and greatly reduced carrier freeze-out on cooling from room temperature, compared to uncapped LAO/STO.[14]

Our sample had dimensions of 5 mm × 5 mm in the xy plane, with electrical contacts made by wire bonding through the top surface in a van der Pauw geometry. Resistance was measured using a standard ac technique with excitation currents of 1 or 2 μA. Experiments were carried out in magnetic fields of up to 20 T, in a pumped ^{3}He system with a rotatable sample stage.

Fig. 1(a)(i) shows the magnetoresistance ρ_{xx} at various temperatures, for magnetic fields aligned perpendicular to the xy plane. Clear oscillations with strongly temperature-dependent amplitudes are apparent, and the complex periodicity indicates that several frequencies are superposed. Fig. 1(a)(ii) shows the same data as in (i), but with a smooth background removed. An example of the background subtracted is shown in the inset. The Hall effect ρ_{xy} showed quantum oscillations similar to those in ρ_{xx}, on a large, approximately linear background (Fig. 1(c)(iii)). Apart from the oscillation amplitudes, ρ_{xy} is independent of temperature. By performing all measurements with both positive and negative magnetic field polarities, and carrying out the usual antisymmetrisation procedure, we exclude the possibility that the oscillatory Hall effect arises from an admixture of ρ_{xx} in ρ_{xy}, or vice versa. Observable quantum oscillations in the Hall effect are relatively unusual, but arise from the same Landau level-related phenomena as SdH oscillations in ρ_{xx}.[6,24,25]

Fig. 1(b) shows the dependence of ρ_{xx} on the angle θ between the magnetic field direction and the z-axis of the sample. The oscillations move out to progressively higher fields as θ is increased, showing that the conduction electrons are confined to the interface plane and quantum oscillations are generated only by the perpendicular component of the applied field. This behaviour confirms the two-dimensionality of the conducting electron system.

In the case of a single occupied 2D subband, the period of SdH oscillations scales with $1/\cos\theta$. When multiple 2D subbands are occupied, however, mixing of Landau quantisation with the confinement potential leads to anti-crossings of discrete levels from different subbands as the field is tilted.[26] Landau level energies therefore show a complicated magnetic field dependence, which progressively modifies the periodicity of SdH oscillations as a function of θ. The data in Fig. 1(b) show a changing periodicity as θ is increased, which can be clearly seen as a function of the perpendicular field component in Fig. 1(c), and further indicates that multiple occupied subbands contribute to transport in this material.

It can also be seen from Fig. 1(b) that the background magnetoresistance changes from positive to negative, and a pronounced drop in the resistance develops at ∼11 T as θ approaches 90°. We suggest that this is related to a decrease in inter-subband scattering as the magnetic field component parallel to the interface shifts the subband energies, as is commonly observed in multi-subband semiconductor 2DEGs.[27–29] The steep drop in ρ_{xx} for parallel field close to 11 T is then associated with depopulation of the highest subband as it crosses the Fermi energy (see the supplementary material for more details[13]).

The oscillations in ρ_{xx} at $\theta = 0°$ have amplitudes of the order of 10% of the total resistance, which suggests that Landau levels are not fully resolved in this system, i.e., there is considerable overlap of

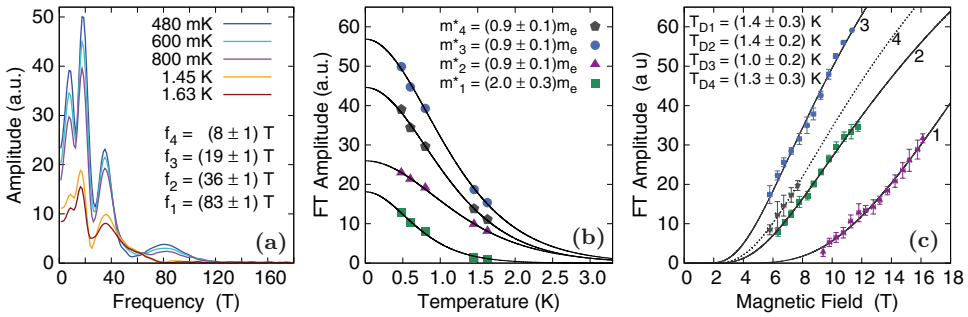

FIG. 2. (a) Fourier transform of SdH oscillations between 4 and 20 T. (b) Temperature dependence of the oscillation amplitudes with values of m^* in units of m_e. The solid lines are fits to $\alpha_i T/\sinh(\alpha_i T)$. Some of the data are rescaled so that all the data can be shown clearly on a single plot. (c) Field dependence of the oscillation amplitudes. The lines are fits to $\exp(-\alpha_i T_{Di})\,\alpha_i T/\sinh(\alpha_i T)$ at 480 mK. The values of T_{Di} extracted from these fits are shown.

levels. This assertion is further supported by the fact that we do not observe the quantum Hall effect, as the presence of SdH oscillations without an accompanying quantum Hall signal indicates that there are extended states between neighbouring Landau levels. In this situation, SdH oscillations are sinusoidal in inverse magnetic field $1/B$, and are described by the general expression,[6,30]

$$\Delta\rho_{xx} = \sum_{i,p} R_{ip} \exp(-\alpha_i T_{D_i}) \frac{\alpha_i T}{\sinh(\alpha_i T)} \sin\left(\frac{2\pi p f_i}{B} + \frac{\pi}{4}\right), \quad (1)$$

where T is temperature, f_i is the frequency of the oscillations corresponding to the ith subband, and p is the harmonic number. R_{ip} is a field- and temperature-independent amplitude, and the other amplitude factors contain the term $\alpha = 2\pi^2 p k_B m^*/\hbar e B$, which allows the effective mass m^* and Dingle temperature T_D of the charge carriers to be extracted from the temperature and magnetic field dependence of the signal.[6] T_D is a measure of the quantum mobility μ, and can be expressed as $T_D = (e\hbar/2\pi k_B)(1/m^*\mu)$.

To analyse the $\Delta\rho_{xx}$ data in Fig. 1(a)(ii), we performed Fourier transforms (FTs) in the inverse magnetic field. Fig. 2(a) gives the resulting Fourier spectra for the field range from 4–20 T, which show four peaks corresponding to four distinct oscillation frequencies in the SdH signal. The frequencies of the peaks are shown in the figure, with errors corresponding to the maximum variation of the peak positions for FTs over different magnetic field ranges.

The very low frequency oscillation, corresponding to the FT peak at 8 T, may be subject to some uncertainty due to the difficulty of achieving perfect background subtraction. However, we found that the FT is robust to small variations in the form of the subtracted background curve. Moreover, the amplitude of the 8 T peak has strong temperature dependence compared to the very weak temperature dependence of the background below 2 K (see Fig. 1(a)), and the background curves we subtracted show no periodic component. We therefore treat the lowest frequency FT peak as a genuine component of the SdH signal. In the absence of harmonic content, which we will discuss below, the FT results indicate that four high mobility conduction subbands contribute to the quantum transport in our sample.

By fitting the temperature dependence of the FT peak amplitudes to $\alpha_i T/\sinh(\alpha_i T)$, we extracted the carrier effective mass for each subband (see Fig. 2(b)). FTs were performed over several overlapping magnetic field ranges, with B calculated as $(0.5\,(1/B_{min} + 1/B_{max}))^{-1}$ for each range. This was repeated for each temperature, and the effective masses were extracted for each field range. The masses quoted in Fig. 2(b) are the mean values of m^* resulting from this procedure. In all cases, the experimental temperature dependence is well-described by the theoretical curves, and the errors given reflect the uncertainty in m^* introduced by Fourier transforming over a wide magnetic field range, rather than the quality of the fits to $\alpha_i T/\sinh(\alpha_i T)$.

Fig. 2(c) shows the magnetic field dependence of the oscillation amplitudes. We performed FTs of the 480 mK $\Delta\rho_{xx}$ data over many overlapping field ranges of varying length, and collected the FT peak amplitudes into bins of 0.5 T width. The data points in the figure represent the bin averages

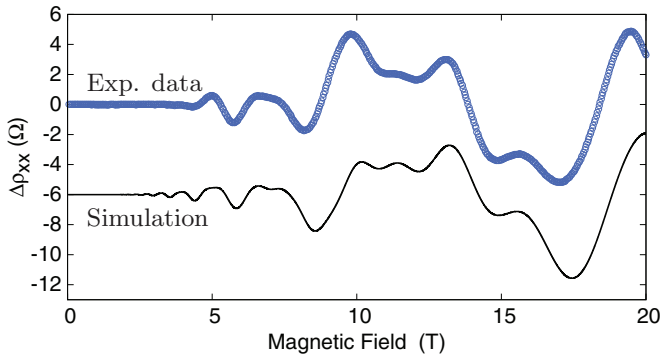

FIG. 3. Comparison of experimental data with a calculation of expression (1) using the values of f_i, m_i^*, and T_{Di} extracted from the Fourier analysis and shown in Fig. 2. Both curves are at 480 mK, the calculated curve is offset from zero.

with x- and y-errorbars of $\pm$ one standard deviation. The Dingle temperature for each subband was then extracted by fitting $A_i \exp(-\alpha_i T_{Di})\,\alpha_i T/\sinh(\alpha_i T)$, where A_i is a constant. The values of T_{Di} obtained are shown in the figure, with errors that incorporate both the scatter of the data and the errors in m_i^*.

We can use our values of T_{Di} and m_i^* to calculate the quantum mobilities of each subband, and find $\mu_1 = 800 \pm 200$ cm^2 V^{-1} s^{-1}, $\mu_2 = 1700 \pm 300$ cm^2 V^{-1} s^{-1}, $\mu_3 = 2400 \pm 500$ cm^2 V^{-1} s^{-1}, and $\mu_4 = 1800 \pm 500$ cm^2 V^{-1} s^{-1}.

If the SdH signal contains harmonics of a given oscillation, the measured frequencies *and* the temperature and field dependence of the amplitudes should scale with the harmonic number p (we actually extract pm_i^* and pT_{Di} from the fits in Figs. 2(b) and 2(c), respectively). This is not the case for any of the oscillations we observe in our samples, and we conclude that the peaks in the FT correspond to fundamental frequencies ($p = 1$), implying independent conduction channels.

As a check of our Fourier analysis, we used the values of f_i, m_i^*, and T_{Di} extracted from the FTs to calculate the SdH signal expected according to expression (1). The constant amplitude factor R_i may depend on the effective mass but should otherwise be the same for each subband (see the supplementary material[13]), so we set $R_2 = R_3 = R_4$, and used R_1 and R_2 as free parameters to fit the amplitude of expression (1) to the $\Delta\rho_{xx}$ data. The result is shown in Fig. 3. The features and overall amplitude of the experimental data are reproduced extremely well by the calculated curve, showing that the results of the Fourier analysis are reliable.

To try to understand the nature of the subbands we observe, we start by considering the conduction bandstructure of bulk STO, which consists of three degenerate bands with minima at the gamma-point of the Brillouin zone, arising from the Ti 3d xy, xz, and yz orbitals. The degeneracy of these bulk bands is lifted by a low temperature structural transition and by spin-orbit coupling,[31] and further splitting into 2D subbands occurs with the introduction of the LAO interface and associated confinement potential. The d_{xy}-derived subbands are symmetric in the interface plane and give circular Fermi surfaces with light masses, whereas $d_{xz/yz}$ subbands are weakly dispersing along one of the in-plane directions, and should lead to elliptical Fermi surfaces with heavy effective masses, perhaps of order 10–20 m_e.[10–12,32]

The masses of $0.9m_e$ and $2m_e$ that we measure, however, are somewhat intermediate between light and heavy, and suggest carriers in hybridised subbands with mixed orbital character, an interpretation supported by recent theoretical work.[33] The differences between masses in different subbands should reflect the degree of hybridisation, and thus depend sensitively on factors such as carrier density and spin-orbit coupling.[33,34]

The hybridised Fermi surfaces associated with the (relatively light) effective masses we measure can be expected to have warped circular symmetry, and for a two-dimensional electron system with circular Fermi surface sections, the frequency f_i of quantum oscillations is proportional to the carrier density in a given subband $n_i = N_v N_s e f_i / h$, where N_v and N_s are valley and spin degeneracy, respectively. We use this relation, assuming a single valley and twofold spin degeneracy, to calculate

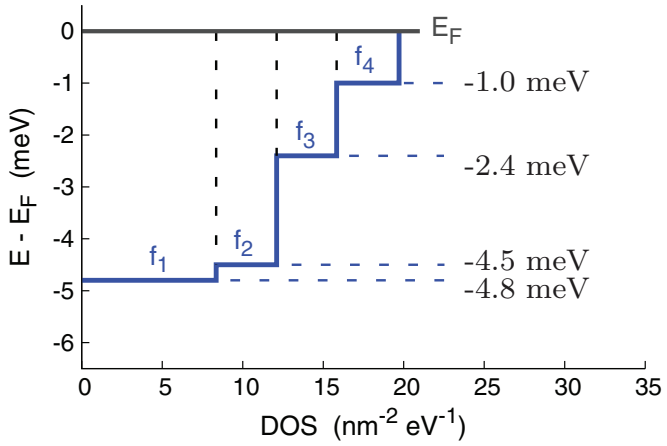

FIG. 4. Density of states (DOS) for the multi-subband 2DEG in our sample.

the carrier densities n_i and hence a total carrier density of $n_{SdH} = \sum_i n_i = (0.71 \pm 0.02) \times 10^{13}$ cm^{-2} contributing to the SdH effect. This is close to the value of $n_{Hall} = 1.0 \times 10^{13}$ cm^{-2} that we extract from the slope of the Hall signal in Fig. 1(a)(iii).[35] We then use the 2D density of states to calculate the energies of the subband edges relative to the Fermi energy, $E_F - E_i = n_i \pi \hbar^2 / m_i^*$, and give the values in Fig. 4, which shows the subband structure of our STO/SCO/LAO/STO sample.

The most striking aspect of this subband structure is the small energy scale involved. The lowest subband edge is only a few millielectronvolts below the Fermi energy, and the separation of the subbands is of order 2 meV or less. We emphasise the observation of this small energy scale, as bandstructure calculations that assume a full electronic reconstruction at the LAO/STO interface,[2,36] and a correspondingly high carrier density of $\sim 3.3 \times 10^{14}$ cm^{-2}, predict energies of at least an order of magnitude larger, in the range of tens to hundreds of meV, for the occupied conduction subbands.[10–12] By contrast, our results are in very good agreement with bandstructure calculations for an LAO/STO 2DEG with carrier density close to the $\sim 10^{13}$ cm^{-2} that we measure.[33,34] This suggests that we have measured (at least) a large majority of the conduction electrons in this 2D system, so that our results provide a strong experimental guideline for understanding the characteristic properties of the charge carriers and the evolution of the conduction bandstructure with the total carrier density of the 2DEG.

Previous measurements on LAO/STO could clearly resolve only a single SdH frequency,[8,9] and so were unable to provide any information about the overall subband structure, but experiments on δ-doped STO[37,38] and electric-field-induced STO 2DEGs[39] imply a subband energy scale similar to the one we measure in STO/SCO/LAO/STO. We note that the closely spaced subband energies we observe are at the limits of resolution for ARPES and related experiments, and may shed light on the failure, so far, to resolve the bandstructure at the LAO/STO interface using these techniques. The relatively weak confining potential implied by the small subband energies (more details in the supplementary material[13]) may also be reflected in the lower than expected core-level shifts observed in photoemission studies.[18,40,41]

In summary, we have measured high resolution SdH oscillations in a STO/SCO/LAO/STO heterostructure, and show that multiple 2D subbands with different effective masses and mobilities, suggesting mixed orbital character, are responsible for conduction. Our results are consistent with previous SdH measurements of a single subband in LAO/STO,[8,9] but the resolution of several additional subbands allows us to confirm a correspondingly higher density of carriers contributing to quantum transport. Measurements in tilted magnetic fields show evidence of inter-subband scattering. We have calculated the energies of successive subband edges, and find a subband structure in very good agreement with bandstructure calculations for low carrier density LAO/STO 2DEGs.

This work was performed at the HFML/RU-FOM member of the European Magnetic Field Laboratory (EMFL), and has been supported by the InterPhase program of the Stichting

Fundamenteel Onderzoek der Materie (FOM) with financial support from the Nederlandse Organisatie voor Wetenschappelijk Onderzoek (NWO). A.M.C. acknowledges support from a Marie Curie IIF grant.

[1] A. Ohtomo and H. Y. Hwang, Nature (London) **427**, 423 (2004).
[2] J. Mannhart, D. H. A. Blank, H. Y. Hwang, A. J. Millis, and J.-M. Triscone, MRS Bull. **33**, 1027 (2008).
[3] N. Reyren, S. Thiel, A. D. Caviglia, L. Fitting Kourkoutis, G. Hammerl, C. Richter, C. W. Schneider, T. Kopp, A.-S. Rüetschi, D. Jaccard, M. Gabay, J.-M. Triscone, and J. Mannhart, Science **317**, 1196 (2007).
[4] A. Brinkman, M. Huijben, M. van Zalk, J. Huijben, U. Zeitler, J. C. Maan, W. J. van der Wiel, G. Rijnders, D. H. A. Blank, and H. Hilgenkamp, Nature Mater. **6**, 493 (2007).
[5] H. Chen, A. M. Kolpak, and S. Ismail-Beigi, Adv. Mater. **22**, 2881 (2010).
[6] D. Shoenberg, *Magnetic Oscillations in Metals* (Cambridge University Press, 1984).
[7] G. Herranz, M. Basletić, M. Bibes, C. Carrétéro, E. Tafra, E. Jacquet, K. Bouzehouane, C. Deranlot, A. Hamzić, J.-M. Broto, A. Barthélémy, and A. Fert, Phys. Rev. Lett. **98**, 216803 (2007).
[8] A. D. Caviglia, S. Gariglio, C. Cancellieri, B. Sacépé, A. Fête, N. Reyren, M. Gabay, A. F. Morpugo, and J.-M. Triscone, Phys. Rev. Lett. **105**, 236802 (2010).
[9] M. Ben Shalom, A. Ron, A. Palevski, and Y. Dagan, Phys. Rev. Lett. **105**, 206401 (2010).
[10] Z. S. Popović, S. Satpathy, and R. M. Martin, Phys. Rev. Lett. **101**, 256801 (2008).
[11] W. Son, E. Cho, B. Lee, J. Lee, and S. Han, Phys. Rev. B **79**, 245411 (2009).
[12] P. Delugas, A. Filippetti, V. Fiorentini, D. I. Bilc, D. Fontaine, and P. Ghosez, Phys. Rev. Lett. **106**, 166807 (2011).
[13] See supplementary material at http://dx.doi.org/10.1063/1.4863786 for details of the sample growth, modeling of the diamagnetic shift for in-plane magnetic field, data from additional samples, and further discussions of spin-splitting and the Hall effect.
[14] M. Huijben, G. Koster, M. K. Kruize, S. Wenderich, J. Verbeeck, S. Bals, E. Slooten, B. Shi, H. J. A. Molegraaf, J. E. Kleibeuker, S. van Aert, J. B. Goedkoop, A. Brinkman, D. H. A. Blank, M. S. Golden, G. Tendeloo, H. Hilgenkamp, and G. Rijnders, Adv. Funct. Mater. **23**, 5240 (2013).
[15] W. Siemons, G. Koster, H. Yamamoto, W. A. Harrison, G. Lucovsky, T. H. Geballe, D. H. A. Blank, and M. R. Beasley, Phys. Rev. Lett. **98**, 196802 (2007).
[16] C. Cancellieri, N. Reyren, S. Gariglio, A. D. Caviglia, A. Fête, and J.-M. Triscone, Europhys. Lett. **91**, 17004 (2010).
[17] S. Thiel, G. Hammerl, A. Schmehl, C. W. Schneider, and J. Mannhart, Science **313**, 1942 (2006).
[18] M. Takizawa, S. Tsuda, T. Susaki, H. Y. Hwang, and A. Fujimori, Phys. Rev. B **84**, 245124 (2011).
[19] C. Bell, S. Harashima, Y. Hikita, and H. Y. Hwang, Appl. Phys. Lett. **94**, 222111 (2009).
[20] E. Breckenfeld, N. Bronn, J. Karthik, A. R. Damodaran, S. Lee, N. Mason, and L. W. Martin, Phys. Rev. Lett. **110**, 196804 (2013).
[21] Y. Xie, Y. Hikita, C. Bell, and H. Y. Hwang, Nature Commun. **2**, 494 (2011).
[22] Y. Xie, C. Bell, Y. Hikita, S. Harashima, and H. Y. Hwang, Adv. Mater. **25**, 4735 (2013).
[23] R. Pentcheva, M. Huijben, K. Otte, W. E. Pickett, J. E. Kleibeuker, J. Huijben, H. Boschker, D. Kockmann, W. Siemons, G. Koster, H. J. W. Zandvliet, G. Rijnders, D. H. A. Blank, H. Hilgenkamp, and A. Brinkman, Phys. Rev. Lett. **104**, 166804 (2010).
[24] J. M. Reynolds, H. W. Hemstreet, T. E. Leinhardt, and D. D. Triantos, Phys. Rev. **96**, 1203 (1954).
[25] N. Doiron-Leyraud, C. Proust, D. LeBoeuf, J. Levallois, J.-B. Bonnemaison, R. Liang, D. A. Bonn, W. N. Hardy, and L. Taillefer, Nature (London) **447**, 565 (2007).
[26] J. C. Maan, in *Springer Series in Solid State Sciences*, edited by G. Bauer, F. Kuchar, and H. Heinrich (Springer, Berlin, 1984), Vol. 53, p. 183.
[27] W. Beinvogl, A. Kamgar, and J. F. Koch, Phys. Rev. B **14**, 4274 (1976).
[28] T. Englert, J. C. Maan, D. C. Tsui, and A. C. Gossard, Solid State Commun. **45**, 989 (1983).
[29] J. C. Portal, R. J. Nicholas, M. A. Brummell, A. Y. Cho, K. Y. Cheng, and T. P. Pearsall, Solid State Commun. **43**, 907 (1982).
[30] I. M. Lifshitz and A. M. Kosevich, Sov. Phys. JETP **2**, 636 (1956).
[31] L. F. Mattheiss, Phys. Rev. B **6**, 4740 (1972).
[32] A. F. Santander-Syro, O. Copie, T. Kondo, F. Fortuna, S. Pailhès, R. Weht, X. G. Qiu, F. Bertran, A. Nicolaou, A. Taleb-Ibrahimi, P. L. L. Fèvre, G. Herranz, M. Bibes, N. Reyren, Y. Apertet, P. Lecoeur, A. Barthélémy, and M. J. Rozenberg, Nature (London) **469**, 189 (2011).
[33] L. W. van Heeringen, G. A. de Wijs, A. McCollam, J. C. Maan, and A. Fasolino, Phys. Rev. B **88**, 205140 (2013).
[34] G. Khalsa and A. H. MacDonald, Phys. Rev. B **86**, 125121 (2012).
[35] We note that significant Fermi surface anisotropy for the most strongly hybridised subbands is a possible source of error in our value of n_{SdH}, and non-parabolicity of the subbands may additionally lead to magnetic field dependence of the effective masses or carrier densities that we have not accounted for (see Ref. 32).
[36] S. Okamoto and A. J. Millis, Nature (London) **428**, 630 (2004).
[37] Y. Kozuka, M. Kim, C. Bell, B. G. Kim, Y. Hikita, and H. Y. Hwang, Nature (London) **462**, 487 (2009).
[38] M. Kim, C. Bell, Y. Kozuka, M. Kurita, Y. Hikita, and H. Y. Hwang, Phys. Rev. Lett. **107**, 106801 (2011).
[39] K. Ueno, S. Nakamura, H. Shimotani, A. Ohtomo, N. Kimura, T. Nojima, H. Aoki, Y. Iwasa, and M. Kawasaki, Nature Mater. **7**, 855 (2008).
[40] K. Yoshimatsu, R. Yasuhara, H. Kumigashira, and M. Oshima, Phys. Rev. Lett. **101**, 026802 (2008).
[41] Y. Segal, J. H. Ngai, J. W. Reiner, F. J. Walker, and C. H. Ahn, Phys. Rev. B **80**, 241107(R) (2009).